



## Anion and cation binding by a new indole/pyridine/amine-based ion-pair receptor

Kristin N. Skala, Katelyn G. Perkins, Amna Ali, Robert Kutlik, Addie M. Summitt, Satyanarayana Swamy-Mruthinti, Farooq A. Khan\*, Megumi Fujita\*

Department of Chemistry and Department of Biology, University of West Georgia, 1601 Maple St., Carrollton, GA 30118, United States

### ARTICLE INFO

#### Article history:

Received 26 July 2010

Revised 30 September 2010

Accepted 3 October 2010

Available online 28 October 2010

#### Keywords:

Indole

Ion-pair receptor

Cation binding

Anion binding

ESI-MS

### ABSTRACT

A new ion-pair receptor bis(3-bromoindol-2-ylmethyl)(2-pyridylmethyl)amine (**1**) was synthesized and studied for its anion and cation binding behavior using ESI-MS and  $^1\text{H}$  NMR spectroscopy. Among halides, **1** exhibits the strongest binding with  $\text{Cl}^-$  to form a 1:1 adduct ( $K_a = 1042 \pm 21$  in  $\text{CD}_3\text{CN}$ ). Among alkali metal ions,  $\text{Li}^+$  and  $\text{Na}^+$  showed the strongest binding in the formation of a  $1\cdot\text{M}^+$  complex. The simultaneous binding of  $\text{Cl}^-$  and  $\text{Li}^+$  to **1** was confirmed by  $^1\text{H}$  NMR titration of a 1:1 mixture of **1** and  $\text{Cl}^-$  with  $\text{LiPF}_6$  in 83:17 v/v mixture of  $\text{CDCl}_3$  and  $\text{DMSO}-d_6$ . DFT-optimized structures of  $1\cdot\text{Cl}^-$ ,  $1\cdot\text{Li}^+$ , and  $1\cdot\text{Li}^+\cdot\text{Cl}^-$  are consistent with the chemical shift changes observed in  $^1\text{H}$  NMR studies.

© 2010 Elsevier Ltd. All rights reserved.

### 1. Introduction

Ion-pair receptors are molecules that are capable of binding both an anion and a cation simultaneously.<sup>1</sup> Such systems have drawn much attention in recent years, and the number of publications on this topic has grown rapidly in the past decade. Ion-pair receptors have potential applications in solubilization and extraction of salts from organic solvents or effluents, in the transfer of salts through lipophilic membranes, and as sensors for biological and environmental systems.<sup>1</sup>

The use of indole groups in anion or ion-pair receptors, along with related carbazoles, biindoles, and indolo[2,3-*a*]carbazoles, is fairly new.<sup>2</sup> The work from 2004 to 2008 on anion receptors with indole motifs is well summarized by Gale,<sup>2</sup> and more recent works are cited in Jeong's recent article on new indolocarbazole-based anion receptors.<sup>3</sup> However, the number of indole-based ion-pair receptors reported to date is still limited.<sup>4</sup> Jeong and co-workers have synthesized a biindole-based ion-pair receptor by coupling biindole with a diazacrown ether, which binds an alkali metal ion and a halide anion cooperatively.<sup>4a</sup> Ito and co-workers reported a series of indolylmethanes that bind anions and ion-pairs.<sup>4b</sup>

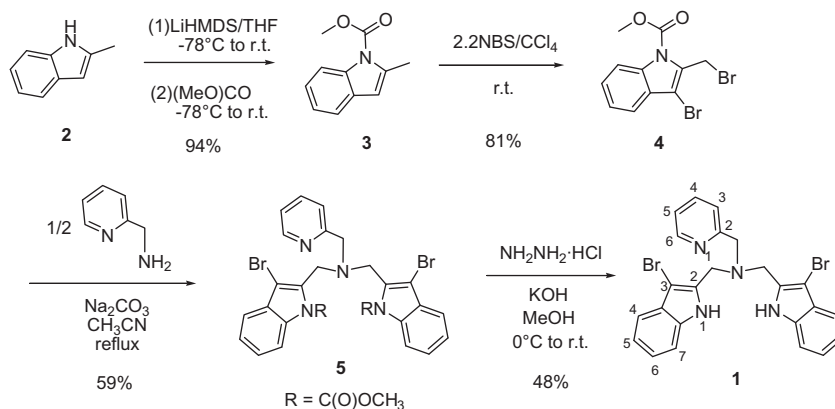
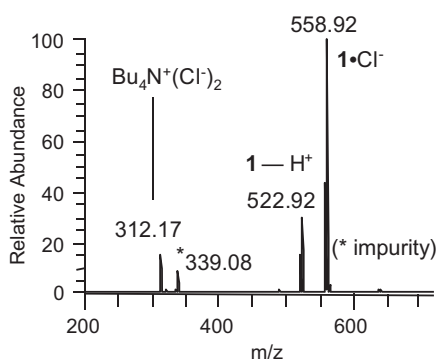
Herein we report a newly synthesized receptor bis(3-bromoindol-2-ylmethyl)(2-pyridylmethyl)amine (**1**, Scheme 1) that is capable of binding both an anion and a cation. This molecule

contains two indole N–H groups that can potentially enable interaction with an anion through hydrogen bonding, and two amine/pyridine N atoms to allow a cation to bind. While it is a common approach to synthesize an ion-pair receptor by functionalizing well-known cation-binding macrocycles such as crown ethers, calixarenes or cholapods,<sup>1a,e</sup> receptor **1** is acyclic and contains a minimal number of cation-binding heteroatoms. The Br groups in the indolyl moieties of **1** are not directly involved in ion binding, yet were included in the synthesis to allow the possibility to substitute one or both with other groups to tune the molecule's electronic properties or to enhance colorimetric responses to ion binding.

The receptor **1** was synthesized in four steps starting from 2-methylindole **2** (Scheme 1). The first two steps, N-protection and dibromination by NBS, were modified from Nagarathnam's procedure.<sup>5</sup> The dibrominated compound **4** was coupled with 2-(aminomethyl)pyridine in 2:1 ratio to give **5** in 59% yield. After N-deprotection of **5**, the final product **1** was obtained (48%).

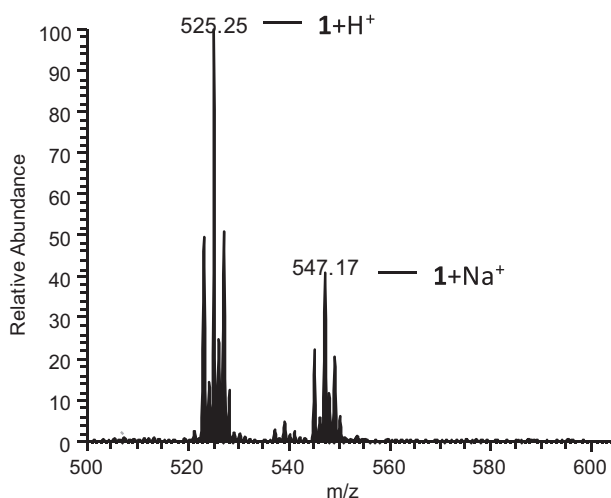
We first examined the halide-binding behavior of **1** in methanol using ESI-MS. A series of methanol solutions of **1** with 5 equiv of  $\text{Bu}_4\text{N}^+\text{X}^-$  ( $\text{X}^- = \text{F}^-, \text{Cl}^-, \text{Br}^-$  and  $\text{I}^-$ ) was used for individual halide-binding assessment. A representative negative-ion mode spectrum with  $\text{Cl}^-$  is shown in Figure 1. This spectrum shows the 1:1 adduct  $1\cdot\text{Cl}^-$  along with signals corresponding to the mono-deprotonated receptor  $[1-\text{H}^+]^-$  and  $[\text{Bu}_4\text{N}^+(\text{Cl}^-)_2]^-$ . Analogous peaks were also found with  $\text{Br}^-$  and  $\text{I}^-$ . With  $\text{F}^-$ , no 1:1 adduct was observed but instead the 2:1 adduct  $(1)_2\cdot\text{F}^-$  ( $m/z = 1067$ ) was detected with a small intensity. The signal intensities of the  $1\cdot\text{X}^-$  species are in

\* Corresponding authors. Tel.: +1 678 839 6024; fax: +1 678 839 6551 (M.F.).  
E-mail address: [mfujita@westga.edu](mailto:mfujita@westga.edu) (M. Fujita).

Scheme 1. Synthesis of **1**.Figure 1. Negative-ion ESI mass spectrum of 1:5 mole ratio of **1**:Cl<sup>-</sup> in methanol.

the order of Cl<sup>-</sup> > Br<sup>-</sup> > I<sup>-</sup>, though for more quantitative comparison we used <sup>1</sup>H NMR titrations as discussed later.

We also examined the Group 1A cation binding to **1** in methanol by ESI-MS. A series of solutions of **1** with 5 equiv of MPF<sub>6</sub> (M = Li, Na and K) or RbBF<sub>4</sub> were used for individual cation-binding assessment. In the positive-ion mode, signals of a 1:1 adduct **1**·M<sup>+</sup> and the protonated receptor (**1** + H<sup>+</sup>) were observed. A sample positive-mode spectrum of a mixture of **1** and Na<sup>+</sup> is shown in Figure 2. Among the first three cations, the **1**·M<sup>+</sup> signal intensities were roughly in the order of Li<sup>+</sup> ~ Na<sup>+</sup> > K<sup>+</sup> though further attempts to

Figure 2. Positive-ion ESI mass spectrum of 1:5 mole ratio of **1**:NaPF<sub>6</sub> in methanol.

determine the relative order were made using <sup>1</sup>H NMR as discussed later. A complex of **1** with Rb<sup>+</sup> was not observed when RbBF<sub>4</sub> was used a Rb<sup>+</sup> source, but when RbF was used as a Rb<sup>+</sup> source a signal of **1**·Rb<sup>+</sup> was found, with the intensity comparable to **1**·K<sup>+</sup>. It is not clear why the BF<sub>4</sub><sup>-</sup> salt prevented the formation of **1**·Rb<sup>+</sup>.<sup>6</sup>

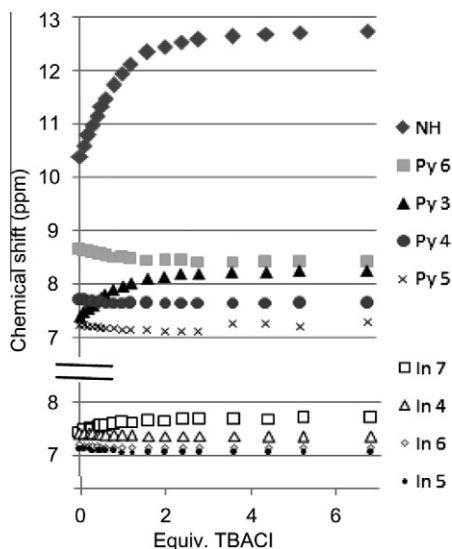
<sup>1</sup>H NMR studies of ion-binding behavior of **1** was carried out in three deuterated solvents: CD<sub>3</sub>CN, CDCl<sub>3</sub>, and an 83:17 mixture (by volume) of CDCl<sub>3</sub> and DMSO-*d*<sub>6</sub>.<sup>7</sup> When **1** was titrated with Bu<sub>4</sub>N<sup>+</sup>Cl<sup>-</sup> in these solvents, notable downfield shift of the NH signal was observed. This indicates that **1** binds Cl<sup>-</sup> through the NH...Cl<sup>-</sup> hydrogen bonding. The titration curves in these solvents all fit to the formation of a 1:1 complex. The association constant *K*<sub>a</sub> (M<sup>-1</sup>) for the formation of **1**·Cl<sup>-</sup> in CD<sub>3</sub>CN, CDCl<sub>3</sub>, and CDCl<sub>3</sub>/DMSO-*d*<sub>6</sub> (83:17) was calculated as 1042 ± 21, 440 ± 23, and 177 ± 18, respectively, using a program WINEQMR2.<sup>8</sup> Association constants in CD<sub>3</sub>CN with other halides were also determined (Table 1). With F<sup>-</sup>, *K*<sub>a</sub> could not be calculated since the chemical shift changes caused by F<sup>-</sup> were so small (Δ0.15 ppm change of the NH signal upon addition of 8 equiv Bu<sub>4</sub>N<sup>+</sup>F<sup>-</sup>). The general order of the *K*<sub>a</sub> values is Cl<sup>-</sup> > Br<sup>-</sup> > I<sup>-</sup> > F<sup>-</sup>, which is consistent with the ESI-MS observation.

Figure 3 shows the movement of chemical shifts of NH and aromatic protons of **1** upon titration with Bu<sub>4</sub>N<sup>+</sup>Cl<sup>-</sup> in CD<sub>3</sub>CN. Upon addition of 6.8 equiv Cl<sup>-</sup>, the NH signal had the most significant downfield shift by +2.35 ppm. The notable downfield shifts were also observed with the pyridyl proton at the 3rd position (Py 3) and the indolyl proton at the 7th position (In 7). These peaks moved by +0.85 and +0.24 ppm, respectively, upon addition of 6.8 equiv Cl<sup>-</sup>, while other aromatic protons hardly moved or only slightly upfield shifted. Similar trend was observed in CDCl<sub>3</sub> and 83:17 CDCl<sub>3</sub>/DMSO-*d*<sub>6</sub> as well. This indicates a possibility of weak hydrogen bonding-like interaction of Py 3 and In 7 protons with the Cl<sup>-</sup>. The DFT-optimized structure of **1**·Cl<sup>-</sup> (Figure 4), obtained by the program GAUSSIAN 09, is consistent with the <sup>1</sup>H NMR observation. The Cl<sup>-</sup> ion is bound by the two indolyl NH groups of **1** in a propeller-like conformation. The NH...Cl<sup>-</sup> distances are 2.14–2.15 Å, clearly within a range of hydrogen bonding.<sup>9</sup> The Py 3 H...Cl<sup>-</sup> and In 7...Cl<sup>-</sup> distances are 2.49 Å and 3.4–3.6 Å,

Table 1

The association constants *K*<sub>a</sub> (M<sup>-1</sup>) of the formation of **1**·X<sup>-</sup> adducts from **1** and Bu<sub>4</sub>NX (X = F, Cl, Br and I) based on titrations of 5 mM of **1** with 50 mM of Bu<sub>4</sub>NX in CD<sub>3</sub>CN.

Halide	F <sup>-</sup>	Cl <sup>-</sup>	Br <sup>-</sup>	I <sup>-</sup>
<i>K</i> <sub>a</sub>	—	1042 ± 21	157 ± 9	12 ± 1



**Figure 3.** Chemical shift movement over titration of **1** with  $\text{Bu}_4\text{NCl}$  in  $\text{CD}_3\text{CN}$ . The pyridyl and indolyl proton signals are shown separately for clarity. See Scheme 1 for numbering of the aromatic protons.

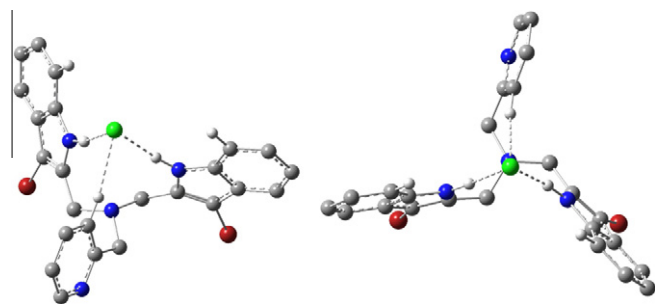


**Figure 4.** Two views of a DFT-optimized structure of  $1\cdot\text{Cl}^-$ . Color scheme: Gray = C, white = H, blue = N, scarlet = Br, and green = Cl. Some hydrogen atoms are omitted for clarity.

respectively. The former is well in the range of reported  $\text{CH}\cdots\text{Cl}^-$  hydrogen bonding distances.<sup>10</sup> Though aromatic CH bonds do not usually form hydrogen bonds, in this case the geometry of  $1\cdot\text{Cl}^-$  brings these protons in proximity of  $\text{Cl}^-$  ion, within a possible range of some interaction.

The interaction between **1** and alkali metal cations from  $\text{MPF}_6$  ( $M = \text{Li}, \text{Na}$  and  $\text{K}$ ) was also examined in  $\text{CD}_3\text{CN}$ , 83:17  $\text{CDCl}_3/\text{DMSO}-d_6$ , and  $\text{CDCl}_3$ . In the first two solvents, addition of 5 equiv  $\text{MPF}_6$  caused very minimal changes (no more than  $\Delta 0.15$  ppm, most peaks moved less than 0.01 ppm) in the  $^1\text{H}$  NMR signals of **1**. Strong coordination of solvent molecules to the cations may be preventing a direct interaction between **1** and  $M^+$ .

In  $\text{CDCl}_3$ , due to poor solubility of  $\text{MPF}_6$ , we could not carry out a titration or quantitative addition of the cation source to **1**. We did a coarse experiment of saturating a 5 mM solution of **1** in  $\text{CDCl}_3$  with  $\text{MPF}_6$  by adding excess solid  $\text{MPF}_6$  and shaking it vigorously. The  $^1\text{H}$  NMR signals of **1** were affected by saturation with  $\text{LiPF}_6$  and  $\text{NaPF}_6$ , but not by  $\text{KPF}_6$ . The chemical shift changes of **1** in  $\text{CDCl}_3$  upon saturation with  $\text{LiPF}_6$  and  $\text{NaPF}_6$  are summarized in Table 2. Interestingly, the NH peak had a significant downfield shift upon addition of  $\text{LiPF}_6$  and  $\text{NaPF}_6$ . This is not due to the hydrogen bonding of the NH groups to the anion  $\text{PF}_6^-$ , since in a separate experiment,  $\text{Bu}_4\text{NPF}_6$  did not cause any changes in proton signals of **1**. The possible reason of the downfield shift of the NH protons is the coordination of the indolyl N atoms to the cation, making the

**Table 2**

Chemical shift changes of proton signals  $\Delta\delta$  (ppm) of **1** in  $\text{CDCl}_3$  upon saturation with  $\text{LiPF}_6$  or  $\text{NaPF}_6$ .

	NH	Py 3	Py 4	Py 5	Py 6	
$\text{LiPF}_6$	+0.78	+0.08	+0.15	-0.25	-0.38	
$\text{NaPF}_6$	+0.78	+0.01	+0.11	-0.21	-0.11	
	In 4	In 5	In 6	In 7	$\text{CH}_2\text{In}$	$\text{CH}_2\text{Py}$
$\text{LiPF}_6$	-0.11	-0.04	-0.09	-0.06	+0.32	+0.17
$\text{NaPF}_6$	-0.06	-0.11	-0.09	-0.002	+0.14	+0.06

NH more electron-deficient. The DFT-optimization of  $1\cdot\text{Li}^+$  indeed resulted in both indolyl N atoms in the coordination sphere of  $\text{Li}^+$ , in addition to the expected pyridyl N and the amine N (Figure 5).

Ion-pair binding behavior of **1** was also examined by  $^1\text{H}$  NMR. In  $\text{CD}_3\text{CN}$ , addition of 4.5 equiv TBACl and 4.5 equiv  $\text{LiPF}_6$  resulted in the precipitate formation ( $\text{LiCl}$  from excess  $\text{Cl}^-$  and  $\text{Li}^+$ ), and the resulting solution matched the spectrum of 1:1 mixture of **1** and  $\text{Cl}^-$  from the titration experiment. Therefore 3.5 equiv of  $\text{LiCl}$  must have precipitated out, and 1 equiv  $\text{Cl}^-$  and 1 equiv  $\text{Li}^+$  must have remained in solution, in which the  $\text{Cl}^-$  ions were interacting with **1**. But apparently  $\text{Li}^+$  in solution does not have any influence on either **1** or the  $1\cdot\text{Cl}^-$  complex. Therefore in  $\text{CD}_3\text{CN}$ , there was no cation binding even by  $1\cdot\text{Cl}^-$ .

On the other hand, we detected evidences of simultaneous binding of  $\text{Cl}^-$  and  $\text{Li}^+$  in 83:17  $\text{CDCl}_3/\text{DMSO}-d_6$ . In Figure 6 the chemical shift changes of proton signals of **1** upon addition of (b) 10 equiv  $\text{Li}^+$ , (c) 10 equiv  $\text{Cl}^-$ , and (d) 10 equiv  $\text{Cl}^-$  and 10 equiv  $\text{Li}^+$  are shown. The changes from (a) to (b), upon addition of  $\text{Li}^+$ , were relatively small, with most notable changes in the two methylene peaks,  $\text{CH}_2\text{In}$  and  $\text{CH}_2\text{Py}$ , by +0.14 and +0.17 ppm. The large changes from (a) to (c) upon addition of 10  $\text{Cl}^-$  in the signals of NH (+1.00 ppm), Py 3 (+0.41 ppm), and In 7 (+0.16 ppm) were consistent with the strong (NH) and weak (Py 3 and In 7) hydrogen bondings to  $\text{Cl}^-$  as discussed earlier. When both 10 equiv  $\text{Bu}_4\text{NCl}$  and 10 equiv  $\text{LiPF}_6$  were added (in either order) to **1** in 83:17  $\text{CDCl}_3/\text{DMSO}-d_6$ , no precipitation occurred, therefore the solution contained 10 equiv each of  $\text{Li}^+$  and  $\text{Cl}^-$ . The proton spectrum of the resulting solution (d) was quite different from **1** only, **1** plus  $\text{Li}^+$ , and **1** plus  $\text{Cl}^-$ . The effect of addition of  $\text{Li}^+$  to the mixture of **1** + 10  $\text{Cl}^-$  (c vs d) is obviously larger compared to the minimal effect of  $\text{Li}^+$  to free **1** (a vs b), indicating that the complex  $1\cdot\text{Cl}^-$  has a significant interaction with  $\text{Li}^+$ , possibly an inclusion of  $\text{Li}^+$ .

However, in the presence of excess of both ions, we cannot ascertain the stoichiometry of  $1:\text{Cl}^-:\text{Li}^+$  in the ternary complex. In order to find the stoichiometry, We titrated a 1:1 mixture of **1** and  $\text{Bu}_4\text{NCl}$  with  $\text{LiPF}_6$  in 83:17  $\text{CDCl}_3/\text{DMSO}-d_6$ . We have already established the 1:1 stoichiometry of the  $1\cdot\text{Cl}^-$  complex based on the titration as discussed earlier. In a 1:1 mixture of **1** and  $\text{Bu}_4\text{NCl}$  a mixture of free **1** and a complex  $1\cdot\text{Cl}^-$  exist, but since we know that the interaction between free **1** and  $\text{Li}^+$  is insignificant, any

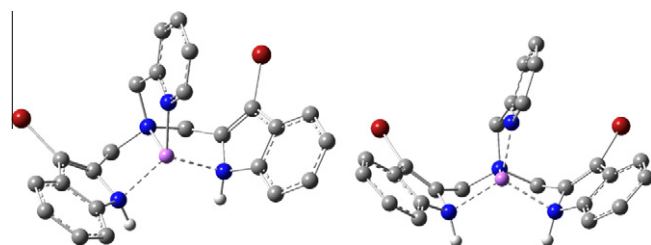


**Figure 5.** Two views of a DFT-optimized structure of  $1\cdot\text{Li}^+$ . Color scheme: Gray = C, white = H, blue = N, and scarlet = Br, and pink = Li. Some hydrogen atoms are omitted for clarity.

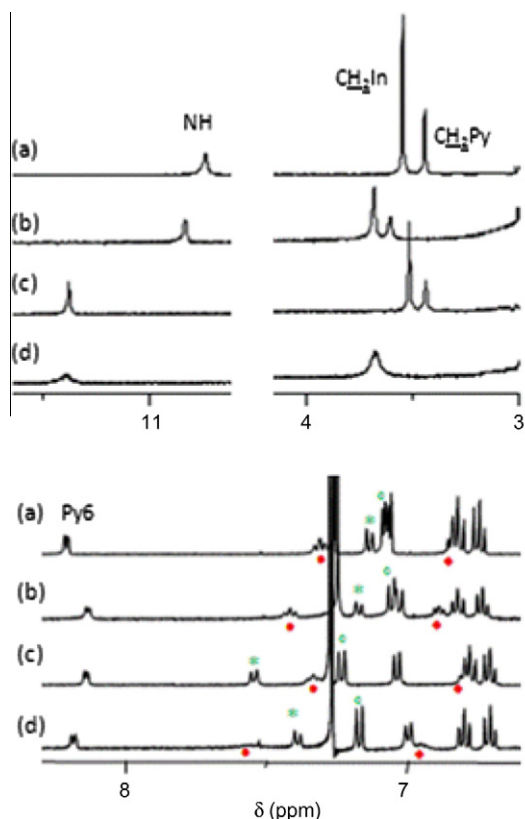


**Figure 6.**  $^1\text{H}$  NMR spectra in 83:17  $\text{CDCl}_3/\text{DMSO}-d_6$  with (a) **1** only, (b) **1** + 10  $\text{LiPF}_6$ , (c) **1** + 10  $\text{Bu}_4\text{NCl}$ , and (d) **1** + 10  $\text{Bu}_4\text{NCl}$  + 10  $\text{LiPF}_6$ .

changes in the  $^1\text{H}$  NMR spectrum can be attributed to the interaction of the  $\mathbf{1}\text{-Cl}^-$  complex with  $\text{Li}^+$ . If the  $\mathbf{1}\text{-Cl}^-$  complex incorporates  $\text{Li}^+$  to form an ion-pair complex  $\mathbf{1}\text{-Cl}^-\text{-Li}^+$ , the equilibrium of  $\mathbf{1}\text{-Cl}^-$  formation ( $\mathbf{1} + \text{Cl}^- \rightleftharpoons \mathbf{1}\text{-Cl}^-$ ) would shift toward the  $\mathbf{1}\text{-Cl}^-$  which would become available for further incorporation of  $\text{Li}^+$ .

The resulting titration curves are presented in Figure 7. The curves of two signals, the NH and the Py 3 proton, had a subtle

'bending' at around 1 equiv point of the  $\text{Li}^+$  addition. As discussed earlier, the NH and Py 3 signals were the most sensitive to the  $\text{Cl}^-$  binding environment due to their hydrogen bonding to  $\text{Cl}^-$ . The bending of the titration curves of these signals is an indication that the nature of the interaction between the  $\mathbf{1}\text{-Cl}^-$  complex and  $\text{Li}^+$  changed at the bending point. The Py 3 peak upfield-shifted up to around 1 equiv point, and then leveled off. The Py 3 peak's upfield shift suggests that the Py 3  $\text{H}\cdots\text{Cl}^-$  hydrogen bonding is weakened by incoming  $\text{Li}^+$ . The level-off of this upfield shift after the 1 equiv point suggests that the  $\mathbf{1}\text{-Cl}^-$  complex is now saturated with 1 equiv of  $\text{Li}^+$ . This supports the formation of an ion-pair complex  $\mathbf{1}\text{-Cl}^-\text{-Li}^+$  with 1:1:1 ratio. Using WINEQNM2,<sup>8</sup> we confirmed that the titration curve up to the 2.5 equiv point fit to the 1:1 equilibrium equation of  $[\mathbf{1}\text{-Cl}^-] + \text{Li}^+ \rightleftharpoons [\mathbf{1}\text{-Cl}^-\text{-Li}^+]$ , and the association constant  $K_a$  was calculated as  $189 \pm 10 \text{ M}^{-1}$ .

The NH signal, on the other hand, had a two-step shape: it downfield-shifted up to 1 equiv, leveled off, and after around 2 equiv point it started to downfield-shift again. The first downfield-shift leveled off at 1 equiv point, but the second downfield-shift was a continuous steady shift up to 15 equiv point (beyond the range shown in the graph). We propose that the first downfield shift is due to incorporation of 1 equiv of  $\text{Li}^+$  to form a ternary complex  $\mathbf{1}\text{-Cl}^-\text{-Li}^+$ , as proposed earlier using the Py 3 titration curve. The curve up to 1.7 equiv point reasonably fit to the 1:1 equilibrium equation of  $[\mathbf{1}\text{-Cl}^-] + \text{Li}^+ \rightleftharpoons [\mathbf{1}\text{-Cl}^-\text{-Li}^+]$  on the WINEQNM2 program's curve fitting. The second downfield-shift is not specific to a certain stoichiometry, and it may be attributed to the excess  $\text{Li}^+$  having less specific interaction with  $\mathbf{1}\text{-Cl}^-\text{-Li}^+$ , such as cation-aromatic  $\pi$  electron interaction. The association constant  $K_a$  based on the NH shift was calculated as  $28 \pm 13 \text{ (M}^{-1})$ . This is sevenfold smaller than the  $K_a$  value calculated based on the Py 3 proton, but the tale end of the 0–1.7 equiv region used for this  $K_a$  calculation was likely to be affected by the secondary non-specific interaction with excess  $\text{Li}^+$ .

Two proposed forms of the ion-pair complex  $\mathbf{1}\text{-Cl}^-\text{-Li}^+$  are depicted in Figure 8. Both structures were DFT-optimized. The first is an intact ion-pair complex (Figure 8a), in which  $\text{Cl}^-$  and  $\text{Li}^+$  are held in proximity, literally an 'ion-pair' binding by **1**. After DFT geometry optimization the resulting structure had a covalent bond between  $\text{Li}^+$  and  $\text{Cl}^-$  with an interatomic distance of 2.24 Å, which is a good match to the calculated and experimental bond distance

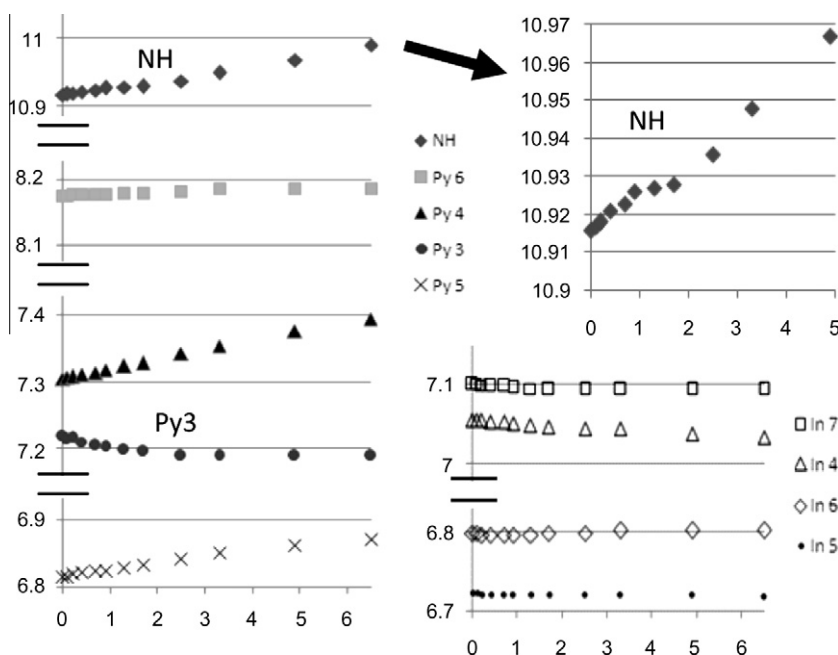


**Figure 7.** Chemical shift movement of  $^1\text{H}$  NMR signals over titration of [**1** + 1 equiv  $\text{Bu}_4\text{NCl}$ ] mixture with  $\text{LiPF}_6$  in 83:17  $\text{CDCl}_3/\text{DMSO}-d_6$ .

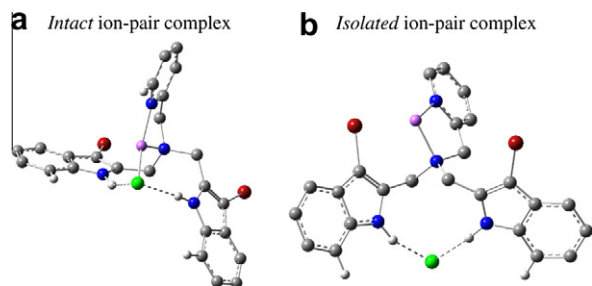


**Figure 8.** DFT-optimized structures of two possible modes of  $1\cdot\text{Cl}^- \cdot \text{Li}^+$ . Color scheme: Gray = C, white = H, blue = N, and scarlet = Br, and pink = Li. Some hydrogen atoms are omitted for clarity.

of a molecule of LiCl, reported as 2.02 Å by Dixon and co-workers.<sup>11</sup> The slightly longer Li $\cdots$ Cl bond distance in  $1\cdot\text{Cl}^- \cdot \text{Li}^+$  is expected since both Li $^+$  and Cl $^-$  ions have other interactions outside of the LiCl core. While both intact and isolated forms are consistent with the  $^1\text{H}$  NMR observation, the former is probably more likely due to the extra stabilization energy from the formation of the Li $\cdots$ Cl bond. Calculations of energies using DFT show that the *intact* complex is more stable than the *isolated* complex by 25 kcal/mol (104 kJ/mol).

In conclusion, we have synthesized a new receptor **1** and demonstrated its ability to bind an anion and a cation separately or simultaneously. Anion binding was generally stronger than cation binding, and among halides the chloride ion had the strongest affinity to **1**.  $^1\text{H}$  NMR titrations were used to show the stoichiometry of the ternary complex  $1\cdot\text{Cl}^- \cdot \text{Li}^+$ .

#### Acknowledgments

Acknowledgment is made to the Donors of the American Chemical Society Petroleum Research Fund for partial support of

this research (Fujita: 45505-GB3; Khan: 50147-URG). Authors are also grateful for NSF MRI grants 0521238 (LC-MS (ESI)) and 00821504 (400 MHz NMR), and the University of West Georgia Technology Fee Grant (GAUSSIAN 09). The authors are grateful to Professor Michael Hynes for his help with the software WINEQNM2.

#### Supplementary data

Supplementary data associated with this article can be found, in the online version, at doi:10.1016/j.tetlet.2010.10.012.

#### References and notes

- For selected reviews, see: (a) Katayev, E. A.; Melfi, P. J.; Sessler, J. L. In *Modern Supramolecular Chemistry: Strategies for Macrocycle Synthesis*; Diederich, F., Stang, P. J., Tykwinski, R. R., Eds.; Wiley-VCH: Weinheim, Germany, 2008; pp 315–347; (b) Gale, P. A.; Garcia-Garrido, S. E.; Garric, J. *Chem. Soc. Rev.* **2008**, *37*, 151–190; (c) Itsikson, N. A.; Geide, I. V.; Morzherin, Y. Yu.; Matern, A. I.; Chupakhin, O. N. *Heterocycles* **2007**, *72*, 53–77; (d) Smith, B. D. In *Ion-pair Recognition by Divalent Receptors, Macrocyclic Chemistry: Current Trends and Future*; Gloe, K., Antonioli, B., Eds.; Kluwer: London, UK, 2005; pp 137–152; (e) Kirkovits, G. J.; Shriver, J. A.; Gale, P. A.; Sessler, J. L. *J. Incl. Phenom. Macrocycl. Chem.* **2001**, *41*, 69–75; (f) Sutherland, I. O. *Adv. Supramol. Chem.* **1990**, *1*, 65–108.
- Gale, P. A. *Chem. Commun.* **2008**, 4525–4540.
- Lee, G. W.; Kim, N.-K.; Jeong, K.-S. *Org. Lett.* **2010**, *12*, 2634–2637.
- (a) Chae, M. K.; Lee, J.-I.; Kim, N.-K.; Jeong, K.-S. *Tetrahedron Lett.* **2007**, *48*, 6624–6627; (b) Nishiki, M.; Oi, W.; Ito, K. *J. Incl. Phenom. Macrocycl. Chem.* **2008**, *61*, 61–69.
- Nagarathnam, D. *Synthesis* **1992**, 743–745.
- $\text{BF}_4^-$  could potentially receive hydrogen bonding from **1** but we did not observe any signal corresponding to  $1\cdot\text{BF}_4^-$ .
- $\text{CD}_3\text{OD}$  and pure  $\text{DMSO}-d_6$  were tested as well, but the  $^1\text{H}$  NMR signals of **1** were not affected upon addition of  $\text{Bu}_4\text{NCl}$  in these solvents. In the former, the NH peak disappeared upon H/D exchange.
- Hynes, M. J. *J. Chem. Soc., Dalton Trans.* **1993**, 311–312.
- Mascal, M. J. *Chem. Soc., Perkin Trans. 2* **1997**, 1999–2001.
- Balamurugan, V.; Hundal, M. S.; Mukherjee, R. *Chem. Eur. J.* **2004**, *10*, 1683–1690.
- Vasiliu, M.; Li, S.; Peterson, K. A.; Feller, D.; Gole, J. L.; Dixon, D. A. *J. Phys. Chem. A* **2010**, *114*, 4272–4281.